Airborne measurements of ground and cloud spectral albedos under low aerosol loads

Ann R. Webb
Physics Department, University of Manchester Institute of Science and Technology (UMIST), Manchester, UK

Arve Kylling
Norwegian Institute for Air Research (NILU), Kjeller, Norway

Manfred Wendisch[1] and Evelyn Jäkel
Leibniz-Institute for Tropospheric Research (IfT), Leipzig, Germany

Received 12 March 2004; revised 16 June 2004; accepted 29 June 2004; published 19 October 2004.

[1] Spectral albedo measurements have been made by three airborne systems (two aircraft and one balloon) over the flat arable land of East Anglia, UK, and above clouds. The spectral albedos measured at the various flight altitudes include the backscattering of the atmosphere beneath the aircraft/balloon, which has to be removed to get the areal spectral surface albedo. Data derived from the airborne spectroradiometers showed the areal surface albedo to be about 0.02 in the UVB (wavelength range between 280–320 nm), increasing with wavelength to about 0.05 at 500 nm. The cloud albedos were measured above two different stratus layers, one completely overcast and one broken. Above the overcast cloud sheet the albedo was independent of wavelength with values between 0.62 and 0.85 depending on position above cloud and altitude. Above the broken cloud layer the averaged albedo spectra showed clear spectral reflection features from the underlying surface mixed with the cloud albedo signatures. *INDEX TERMS:* 3359 Meteorology and Atmospheric Dynamics: Radiative processes; 0360 Atmospheric Composition and Structure: Transmission and scattering of radiation; 0394 Atmospheric Composition and Structure: Instruments and techniques; 3360 Meteorology and Atmospheric Dynamics: Remote sensing; *KEYWORDS:* spectral albedo, cloud albedo, UV/visible, spectroradiometry, airborne platforms, radiative transfer models

Citation: Webb, A. R., A. Kylling, M. Wendisch, and E. Jäkel (2004), Airborne measurements of ground and cloud spectral albedos under low aerosol loads, *J. Geophys. Res.*, *109*, D20205, doi:10.1029/2004JD004768.

1. Introduction

[2] The albedo of any surface is the ratio between the upwelling irradiance reflected from the surface and the downwelling irradiance incident on the surface. It can be specified as a broadband, wavelength-averaged value for the total solar spectrum (300–5000 nm wavelength), for a designated narrower wave band or specific wavelengths (spectral albedo). Most measurements of spectral UV albedo (280–400 nm wavelength) have been made close to the surface [*Feister and Grewe*, 1995; *McKenzie and Kotkamp*, 1996; *Webb et al.*, 2000] and give the reflectivity of a small (uniform) area. However, for radiative transfer modeling purposes the overall albedo of a wider area is needed (approximately 40 km in radius [see *Degünther et al.*, 1998; *Degünther and Meerkötter*, 2000; *Mayer and Degünther*, 2000], requiring knowledge of local land types and their albedos. This quantity is called the areal surface albedo [*Webb et al.*, 2000; *Wendisch et al.*, 2004].

[3] The areal surface albedo is a strong function of e.g. season of the year and specific location. Therefore it should be determined for each radiation measurement campaign separately [*Wendisch and Mayer*, 2003]. In this paper albedo measurements are reported which were conducted in order to analyze radiation data collected within the INSPECTRO (Influence of clouds on the spectral actinic flux in the lower troposphere) project. This experiment took place near Norwich, England, during September 2002. The overall objective of INSPECTRO is to study how clouds alter the vertical profile of actinic flux densities, and hence photolysis frequencies of species relevant to tropospheric photochemistry. During the ground and airborne campaign a number of radiation and microphysical parameters (aerosol particles, cloud droplets) were measured in order to study how clouds modify the radiation field. Also a number of one-dimensional (1-D) and three-dimensional (3-D) radiative transfer models were applied in order to realistically describe these cloud radiative effects. One of the inputs required for the radiation models is the surface albedo, which was determined during some of the flights for the project.

[4] Reported below are comparisons of spectral measurements of albedo made by three airborne instruments.

[1]Now at NASA Ames Research Center, Moffett Field, California, USA.

0148-0227/04/2004JD004768

These are the NILU-CUBE (a cube shaped instrument) suspended below a hot air balloon, a scanning spectroradiometer aboard a Cessna 182 light aircraft and the so-called albedometer (a fixed-grating spectrometer) installed on a Partenavia P68B aircraft. The measured albedos are also compared with simulations from one-dimensional radiative transfer modeling.

[5] In order to derive the surface albedo from the albedo measured at altitude one must remove the effect of the atmosphere between the surface and measurement altitude. *Wendisch et al.* [2004] describe one correction method that requires detailed knowledge of the aerosol beneath the flight altitude, information that is not always available. Here we show that in a clean atmosphere a much simpler method, requiring only albedo measurements from several altitudes, may be used.

2. Experimental Details

2.1. NILU-CUBE, Balloon Borne

[6] The NILU-CUBE [*Kylling et al.*, 2003] has six optical inlets (sensor heads) mounted on the faces of a cube with opposing sensor heads separated by 18 cm. Each sensor head measures the irradiance in two spectral channels centered at approximately 312 and 340 nm wavelength with a full width at half maximum (FWHM) of approximately 10 nm. The spectral response of each individual filter was provided by the filter manufacturer, and the spectral response of one of the assembled heads was independently measured. The filters are all from the same production batch and agree within the manufacturing specifications (center wavelength ±1.5 nm and FWHM ±2 nm). During flight conditions the NILU-CUBE is mounted such that one sensor head faces upward measuring the downwelling radiation. The opposite sensor head measures the upwelling radiation while the remaining four sensor heads point toward the horizon in four opposite directions.

[7] The calibration of the NILU-CUBE is a two-step process. First, the relative variations between the various sensor heads are established by comparing each head with a colocated NILU-UV instrument. Second, one of the sensor heads is absolutely calibrated against a calibrated spectroradiometer. A NILU-UV six channel moderate bandwidth filter radiometer [*Høiskar et al.*, 2003] is used to check the NILU-CUBE calibration before and after flying.

[8] The NILU-CUBE and NILU-UV were intercompared at Norwich Airport on day 261 (2002). Each head of the NILU-CUBE was in turn leveled, and made measurements simultaneously with the NILU-UV for a few minutes. For each sensor head this was repeated 2–4 times. The ratio of the various sensor heads to the upward looking sensor head was established. The dark current was also measured for the various sensor heads and channels and was subtracted from the raw signal prior to calibration. The error in the transfer between the various heads is estimated to be less than 1%.

[9] The procedure outlined by *Dahlback* [1996] was used for the absolute calibration. This includes operation of the NILU-CUBE next to a calibrated spectroradiometer that scans the wavelength region covered by the NILU-CUBE channels. Stable sky conditions are required since the sampling times of the two instruments are different. During the INSPECTRO camp he NILU-CUBE was operated next to the University of Innsbruck spectroradiometer located at Weybourne on day 263. The sky was overcast, but conditions were stable during the 2–4 minutes it takes to scan the wavelength region between 312 and 340 nm. The uncertainty in the transfer of calibration from the University of Innsbruck spectroradiometer to the NILU-CUBE instrument is estimated to be less than 1%. No appreciable drift was found in the NILU-CUBE since its last calibration against the same instrument in Nea Michaniona, Greece, August 2000 [*Webb et al.*, 2002].

[10] The NILU-CUBE was flown suspended beneath a hot air balloon (Cameron Viva 77). After take off the cube was lowered from the side of the balloon basket to several meters below the point at which no further perceivable change occurred in the signal from the top (upward pointing) channel. At this distance (40 m) the cube was assumed to be uninfluenced by the balloon above it. Radiative transfer modeling for the conditions of the flight indicate that the influence of the balloon at this distance would decrease the signal from the upward pointing sensor by 2–3%, a situation that would be little improved within the practical limits of further lowering the cube. The latitude, longitude and altitude of the flight were recorded by a Garmin 12XL GPS logged on a Psion 5. The cube was returned to the balloon basket before landing. The NILU-CUBE suspended beneath the balloon is sufficiently heavy to hang vertically (i.e., the top and bottom surfaces are horizontal) and since the balloon moves at the same speed as the surrounding air there is no effective wind to upset this equilibrium. The cube does rotate in flight but this has no effect on the measurements under discussion.

2.2. Optronic 742 Aboard Cessna 182 Airplane

[11] The Optronic 742 is a wavelength-scanning spectroradiometer mounted in a temperature stabilized box and installed on a Cessna 182 light aircraft. The instrument deployment has been described by *Webb et al.* [2000]. In brief, a bifurcated fiber is used to sample the irradiance from upward and downward pointing cosine response input optics. The signal from up and down pointing fibers is alternated at the entrance slit to the double monochromator so that as the instrument scans the sampling sequence is λ_1(up), λ_1(down), λ_2(up), λ_2(down), ..., λ_n(up), λ_n(down), with λ representing wavelength. The monchromator has a spectral slit function with a FWHM of 1.5 nm. During this project the scans were in 10 nm steps from 300 nm to 500 nm. The time taken for one scan (up and down) is less than 2 minutes, during which time the aircraft traveled approximately 7 km. Occasionally the monochromator was set to a single wavelength and alternated continuously between the upward and downward inputs at the designated wavelength.

[12] The Optronic 742 was calibrated using a 200 W transfer standard traceable to NIST (National Institute for Standards and Technology), and was intercompared with other spectroradiometers twice during the INSPECTRO campaign. An initial intercomparison of all spectroradiometers involved took place in the first week of September, including the University of Innsbruck and Joint Research Centre (JRC) spectroradiometers. The JRC spectroradiometer was also used for intercomparison at Norwich airport (with Optronic 742 installed in the aircraft) on day 262. The instrument was stable during the campaign. Absolute mea-

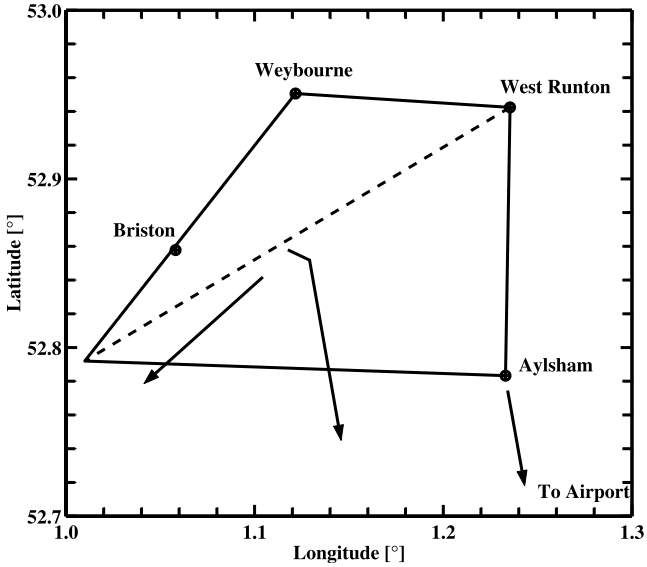

Figure 1. The flight tracks for albedo measurements. The circuit (solid line) is that followed by the Cessna and Partenavia. The dashed diagonal is the track of the Cessna when flying above cloud on 13 September. The arrows are the flight paths of the balloon on 17 September (left) and 20 September (right), respectively. Weybourne and West Runton are on the north Norfolk coast which runs approximately west to east in this area.

surements were about 5% lower than those of the JRC instrument and 8% lower than the University of Innsbruck spectroradiometer, while the JRC instrument was measuring 3% lower than the Innsbruck one. Note, however, that for the albedo measurements (the ratio of downward pointing to upward pointing measurements) it is the relative stability between the two input channels that is important, rather than the absolute calibration. In addition to the absolute temporal stability checks, the relative stability of the channels was checked between flights and found to be constant throughout the project. The wavelength alignment of the monochromator was also frequently checked using a mercury lamp and was within 0.1 nm.

2.3. Albedometer on Partenavia P68B Airplane

[13] The albedometer measures upwelling and downwelling spectral irradiances. It consists of two components: A horizontal stabilization system and an irradiance measurement unit including two separate radiation sensors. The optical inlets (cosine angular response collectors) of both sensors are mounted at the top and the bottom of a Partenavia P68B aircraft and are actively stabilized in a horizontal position with respect to the Earth-fixed coordinate system during the flight.

[14] Each of the two optical inlet systems is connected via fiber optics with a MCS (MultiChannel Spectrometer, manufactured by Zeiss GmbH, Jena, Germany) module, consisting of a fixed grating for wavelength splitting and a 1024 pixel diode array (designed to cover the spectral range between about 290 and 1000 nm wavelength) for simultaneous detection of the spectral radiation. The use of a fixed grating instead anning spectrometer enables a higher time resolution of the measurements (usually 0.3 s) and assures temporal wavelength stability. Both spectrometers have been calibrated in absolute irradiance units (W m^{-2} nm^{-1}) using a 1000 W tungsten halogen lamp (Manufactured by OMTec GmbH, Teltow, Germany, lamp 28), which is traceable to an absolute level (PTB-SL 144) maintained at PTB (Physikalisch-Technische Bundesanstalt, Braunschweig, Germany) with an absolute accuracy of ±3% in the wavelength range between 400–770 nm and ±5% in the spectral regions below 400 nm and above 770 nm. For the wavelength range covered by the spectrometers of the albedometer the stray light contribution is negligible. The wavelength calibration of the two multichannel spectrometers has been confirmed using mercury lamps. The absolute wavelength accuracy is given by the manufacturer to be less than 0.3 nm.

[15] The FWHM of the spectrometers has been determined by exposing the two MCS modules of the albedometer to the spectral radiation emitted by several gas lamps (Hg, Ne, Kr, Xe, Ar). These lamps have distinct and very narrow spectral peaks distributed within the spectral range of the albedometer (Hg: 253.651 and 435.834 nm; Ne: 703.241 nm; Kr: 760.154 and 811.290 nm; Xe: 881.941 nm; Ar: 912.297 nm). The spectral response of the MCS modules was fitted to a Gaussian function type from which the FWHM values are obtained. Values of FWHM between 1.8 and 3.5 nm depending on the specific wavelength were measured by this procedure. The average value of FWHM = 3.0 nm will be used in the data analysis.

[16] The uncertainty for the spectral irradiance measurements was estimated to be ±4% for wavelengths between 400–770 nm and ±6% for wavelengths less than 400 nm and larger than 770 nm.

[17] The albedometer participated in the intercomparison with the JRC instrument performed at the Norwich airport. In the wavelength range 400–500 nm (500 nm being the upper limit of the JRC data) the comparison showed a spectrally flat ratio compared to the JRC instrument, measuring about 4% lower than the JRC data, and very similar to the Optronic results on board the Cessna. At UV wavelengths the ratio of the albedometer data to JRC measurements varied from −20% at 300 nm to +15% at 350 nm wavelength.

[18] Details of the albedometer are described elsewhere [*Wendisch et al.*, 2001; *Wendisch and Mayer*, 2003]. Recently the albedometer has been extended to measure spectral actinic flux densities in addition to spectral flux densities [*Jäkel et al.*, 2004].

2.4. Flight Patterns

[19] Two balloon flights are reported here, which were performed in the late afternoons of days 260 (1655–1725 UTC) and 263 (1615–1705 UTC). On both days the sky was completely overcast with reasonably homogeneous cloud layers and estimated cloud base heights between 2.5 and 3.5 km. The flight tracks ran approximately NE-SW and N-S on days 260 and 263, respectively, and were within the tracks flown by the two aircraft and marked by ground stations used in the INSPECTRO project (see Figure 1). On day 260 most of the flight was at an altitude of about 0.55 km, while on day 263 a slow ascent was made to 1.4 km, followed by a descent and leveling out at 0.7 km.

Table 1. Flight Information for the Three Aircraft

Day of Year	Date (2002)	Flight Times, UTC	Solar Zenith Angle (SZA)	Flight Altitude	Cloud Conditions
256 (Cessna)	13 Sept.	1100–1230	50.3–49.8°	5000 feet (1525 m)	above cloud layer, 5-7/8 Sc below
256 (Partenavia)	13 Sept.	1310–1530	53.4°–53.8°	1600 m	above cloud layer, 4/8 Sc
256 (Partenavia)	13 Sept.	1310–1530	62.9°–62.4°	2800 m	above cloud layer, 4/8 Sc
257 (Partenavia)	14 Sept.	0955–1240	50.0°–51.7°	1600 m	above cloud layer, 8/8 St
257 (Partenavia)	14 Sept.	0955–1240	47.9°–48.1°	2800 m	above cloud layer, 8/8 St
260 (balloon)	17 Sept.	1655–1725	79.9°–84.4°	1800 feet (550 m)	below reasonably homogeneous stratus 8/8 St
263 (Cessna)	20 Sept.	0900–1020	62.5°–55.1°	2200 feet (670 m); 1200 feet (370 m)	below reasonably homogeneous stratus 7/8 St
263 (balloon)	20 Sept.	1615–1705	75.2°–82.5°	5600 feet, 2300 feet, ascent then descent (1700 m, 700 m)	below reasonably homogeneous stratus 8/8 St
268 (Cessna)	25 Sept.	1125–1355	54.0°–60.1°	3000 feet (910 m); 1800 feet (550 m)	blue sky with some Ci 2/8 Ci

[20] The results from three Cessna and two Partenavia flights are discussed here. On days 263 and 268 the Cessna flew circuits around the ground stations marked in Figure 1, flying anticlockwise. On day 256 a diagonal track was flown by the Cessna aircraft back and forth across the box. The Partenavia flew horizontal flight tracks around the measurement area at different altitudes on day 256 and 257.

[21] The tracks flown by the two aircraft are shown in Figure 1; further details are given in Table 1. The ground stations at Weybourne and West Runton (Figure 1) are on the coast, which runs approximately W-E at this point. To the north of this line was sea, to the south was land of predominantly agricultural use with small villages and occasional small areas of woodland. The land is flat with large arable fields and at the time of the flights covered several stages of growth from ploughed field to full crop and the stubble from cut crop. On a small scale it could be classed as variable vegetated or rural land while from a height it appeared as a uniform patchwork. For the purposes of radiative transfer modeling it is the areal albedo that is required, i.e., that of the patchwork rather than immediately above the surface of a single field.

3. Radiative Transfer Simulations

[22] The "uvspec" model from the libRadtran package (http://www.libradtran.org) was used to simulate the radiation measurements. The radiative transfer equation was solved by the discrete ordinate algorithm by *Stamnes et al.* [1988] operating in 16 streams mode with spherical correction as described by *Dahlback and Stamnes* [1991]. The radiative transfer model has compared well with surface UV irradiance measurements [*Mayer et al.*, 1997; *Kylling et al.*, 1998] and airborne tropospheric actinic flux density measurements [*Hofzumahaus et al.*, 2002].

[23] The input to the model comprises the ozone and temperature profiles, surface albedo and altitude and SZA. In addition aerosols and clouds were included in the simulations where noted. Here the ozone profile was taken from the U.S. standard atmosphere model of *Anderson et al.* [1986]. It was scaled to the total ozone column measured by the Total Ozone Mapping Spectrometer. The aerosol amount was around 0.05–0.15 2 nm during the flights presented here. For the simulations the aerosol optical depth was specified using the Ångstrom formula with $\beta = 0.044$ and $\alpha = 1.3$. This gives an optical depth of 0.1 at 532 nm. The aerosol single scattering albedo was set to 0.98. The Heyney-Greenstein phase function was used with an asymmetry factor of 0.75. For the balloon flights a cloud was included between 3 and 4 km. The water cloud optical depth was set to 20 and 15 on days 260 and 263 respectively. The other cloud optical properties were taken from *Hu and Stamnes* [1993]. Solar zenith angle changes during the flights were accounted for. For the Partenavia simulations the effective droplet radius and liquid water content was taken from in situ measurements made by the aircraft. The ozone cross section was taken from *Bass and Paur* [1985]. The SUSIM Atlas-3 extraterrestrial spectrum (ftp://susim.nrl.navy.mil/pub/atlas3/) was used and the Earth-Sun distance was corrected for.

4. Results

4.1. Measurements and Simulations of Airborne Spectral Albedo Measurements and Estimates of Spectral Areal Surface Albedo

[24] The airborne instruments measure the spectral albedo (at a certain altitude above ground) as the ratio of the irradiance incident at the downward pointing sensor head to the irradiance incident on the upward looking sensor head. Since there is a layer of atmosphere between the surface and the actual place of measurement (aircraft or balloon), the spectral albedo at a certain altitude above ground is a combination of the inhomogeneous albedo of the surface and reflection by the intervening atmospheric layer.

[25] Figure 2 shows the spectral albedo measured at 312 and 340 nm wavelength during the two balloon flights, as a function of altitude. The spectral albedo is greater at 312 nm than at 340 nm wavelength, an effect caused by the λ^{-4} dependence of Rayleigh scattering in the atmosphere beneath the flight altitude. This wavelength-altitude effect increases with altitude. The wavelength dependence of the atmospheric influence is further illustrated by the spectral measurements made from the aircraft (Figure 3). In this case the spectral albedo generally increases with wavelength at the lowest flight altitude (0.37 km), in a similar way to spectral

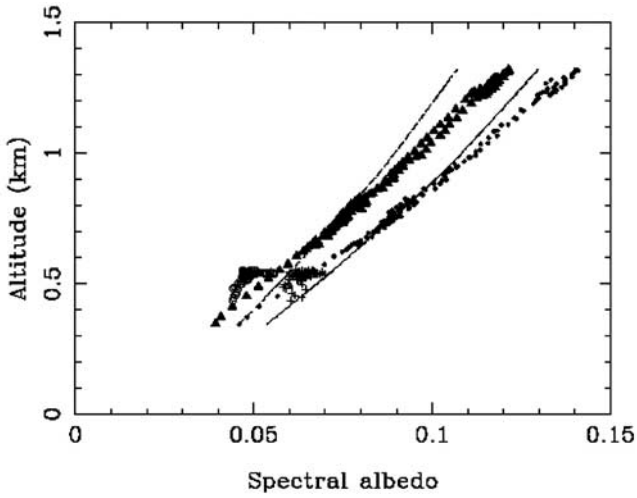

Figure 2. The spectral albedo at 312 (triangles and circles) and 340 nm (dots and crosses) as a function of altitude. The albedo is derived from balloon measurements made on days 260 (circles and crosses) and 263 (triangles and dots). Model simulations are shown as dashed (312 nm) and solid (340 nm) lines.

albedos measured at the surface [*Feister and Grewe*, 1995; *Webb et al.*, 2000]. As flight altitude increases the atmospheric effect, with an opposing wavelength dependence, becomes more influential and the albedo decreases with wavelength at higher altitudes, an effect that has been observed before [*Webb et al.*, 2000; *Wendisch et al.*, 2004].

[26] The peak in the data at around 310 nm wavelength (Figure 3) has also been observed by *Wendisch et al.* [2004] and can be reproduced by radiative transfer modeling. The reason for the peak is a combination of Rayleigh scattering, which decreases as the wavelength increases, and the effect of ozone absorption, which also decreases as the wavelength increases. However, the two effects act in opposite directions in terms of atmospheric transmission and the balance between the two influences results in the peak in measured albedo at a wavelength of about 310 nm. As the simulations show, the peak actually moves to shorter wavelengths as the altitude at which the albedo is measured decreases. However, the temporal resolution of the Cessna albedo measurements is not sufficient to show this over the small altitude range sampled.

[27] Most albedo measurements were made over land, but at 0.91 km the flight leg from West Runton to Weybourne was made about 2 km off the coast so that the majority (all but incident angles of 65°–90°, cosine weighted, on one side) of the field of view of the downward pointing diffuser was viewing the sea (Figure 3). The spectral albedo is higher than that over land, at the same altitude, and so the areal water albedo is greater than that of the adjacent land for each particular wavelength.

[28] The model simulations of spectral albedo are also shown in Figure 2. They were made with a Lambertian surface albedo of 0.02. Thus both model simulations when extrapolated to the ground will yield a surface albedo of 0.02. The extrapolated areal surface albedo estimated by linear extrapolation of t s in Figure 2 to the surface are consistent with a value of 0.02 ± 0.01 for both wavelengths. This value is in agreement with the surface albedo reported by *Feister and Grewe* [1995] for similar surface types and wavelengths. The aircraft albedo measurements for the four flight altitudes are shown as black stars, for 310 nm wavelength with the cube data of 312 nm, and at 340 nm wavelength to match the other cube channel. The aircraft measurements were made at lower SZAs, and for the data from 0.55 km and 0.91 km under blue skies rather than overcast, yet the data still match well with the model and balloon data, especially at 340 nm where the sampling wavelengths are closest.

[29] Figure 2 suggests that a simple linear extrapolation of the flight data of the spectral albedo to the surface will provide the areal spectral surface albedo with sufficient accuracy in this specific measurement case. Therefore, instead of the nonlinear extrapolation technique by *Wendisch et al.* [2004], the use of a linear extrapolation is justified here. This is especially true for the cases with relatively low aerosol optical thickness during the INSPECTRO campaign, whereas the nonlinear extrapolation is required for large aerosol turbidity.

[30] At longer wavelengths suitable albedo measurements to retrieve the areal surface albedo from linear extrapolation to the ground are only available from the spectroradiometer on board the Cessna aircraft (no balloon data), and thus from only four flight altitudes. An example of the linear surface extrapolation of the measured spectral albedo is shown in Figure 4 for the wavelengths of 380 and 480 nm. The values for the areal spectral surface albedo obtained by linear surface extrapolation are given in Table 2. The uncertainty in the surface albedos from such an extrapolation is approximately 0.01 based on the error bars in Figure 4, with correlation coefficients r^2 of 0.95.

[31] The expected general trend of an increase in the extrapolated areal albedo at the surface with increasing wavelength becomes obvious from Table 2. This is com-

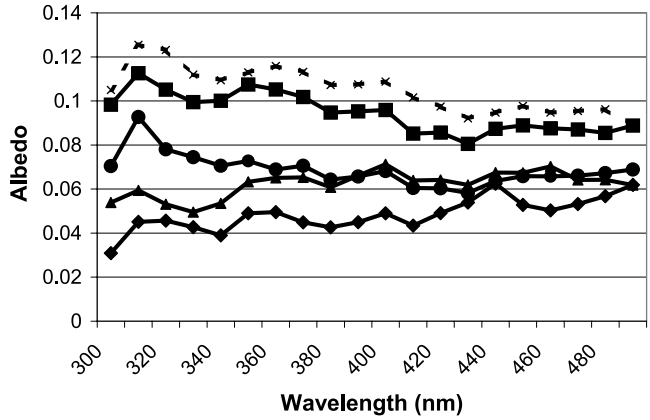

Figure 3. Spectral albedos measured by the Cessna. The data are average values from all the scans made at a given height. The number of scans used in the averaging ranged from 2 (over the sea) to between 6 and 10 for the overland altitudes. Flights were at 370 m (stars), 550 m (triangles), 670 m (circles), 910 m (squares), and 910 m off the coast (dashed line). For reference the balloon went to a maximum altitude of 1400 m.

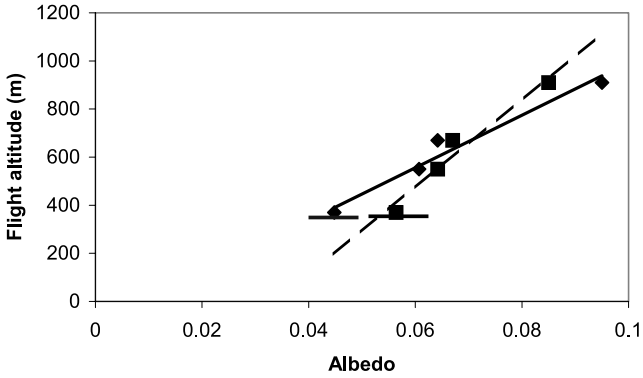

Figure 4. Albedo measurements at four heights from the Cessna and linear extrapolation at 380 nm (solid line) and 480 nm (dashed line). Each data point is the average of several measurements as the aircraft flew around the circuit in Figure 1 on two separate days. Error bars indicate the standard deviations.

mensurate with what one would expect from the agricultural landscape, given the albedos that have been measured for various crop and surface types in the past [*Feister and Grewe*, 1995; *Webb et al.*, 2000]. The areal surface albedo measurements derived from the NILU-CUBE beneath the hot air balloon, and the spectroradiometer on board the Cessna agree within their respective uncertainties, giving confidence in both systems.

[32] At the shorter wavelengths and in the conditions prevalent during the experiment, the linear extrapolation to obtain the areal surface albedo is sufficient, due to a number of factors. In the work by *Wendisch et al.* [2004] the error in surface albedo due to assuming a linear extrapolation reduces as wavelength decreases until the two cannot be separated within the uncertainty of the measurements at UVB wavelengths. It is in this region of reduced nonlinear effects that the NILU-CUBE and spectroradiometer are working. In addition, the flight altitudes were all relatively small and the atmosphere clean compared to the higher altitudes and high turbidity experienced by *Wendisch et al.* [2004]. Thus, in clean air at low altitudes and for UV/visible wavelengths a simple linear extrapolation to the ground appears adequate, but in alternate situations nonlinearity must be considered.

Table 2. Areal Spectral Surface Albedo Calculated by Linear Extrapolation to the Surface of Measured Spectral Albedos From Four Different Altitudes

Wavelength, nm	Extrapolated Areal Surface Albedo
300	0.00 (±0.01)
310	0.004
320	0.003
330	0.004
340	0.006
350	0.006
360	0.007
370	0.009
380	0.009
390	0.010
400	0.012
410	0.018
420	0.020
430	0.025
440	0.034
450	0.033
460	0.029
470	0.029
480	0.036
490	0.038

4.2. Measurements and Simulations of Spectral Cloud Albedo

4.2.1. Scattered Cloud Layer

[33] On day 256 (13 September 2002) the Cessna was flying over a cloud layer with cloudless conditions above. The cloud layer was a reasonably homogenous stratocumulus sheet with a cloud base at about 560 m (1800 ft) altitude and approximately 400 m (1300 ft) depth. The aircraft was flying at an altitude of 1525 m, back and forth along a diagonal track from West Runton to the turning point SW of Briston (Figure 1). The cloud was not a solid layer and there were some breaks in it through which the ground could be seen. These gaps were larger inland toward the turning point past Briston, while toward the coast and West Runton the cloud cover was almost complete before ending abruptly just offshore.

[34] The diagonal circuit was flown twice between 1146 and 1220 UTC, which is four tracks from SW to NE and four tracks from NE to SW. Two scans were made along each track, giving a total of 8 spectra above this cloud layer. The diffuser mounts for the spectroradiometer are designed to be horizontal when the aircraft is in its normal attitude for level flight. On day 256 the flight attitude was not quite as normal and the aircraft logging system showed a pitch angle of 2°–3° (slightly nose up). This resulted in two different values for the downwelling irradiance from the clear sky above, so for the calculation of albedo the average value has been taken for all scans. The aircraft attitude would also have affected the measurement of the upwelling irradiance, but this effect is masked by the far greater variability caused by the changing gaps in the underlying cloud. Figure 5 shows three examples of the measured spectra for cloud albedo representing the natural variability of the cloud albedo in this case. The highest value is from a scan made

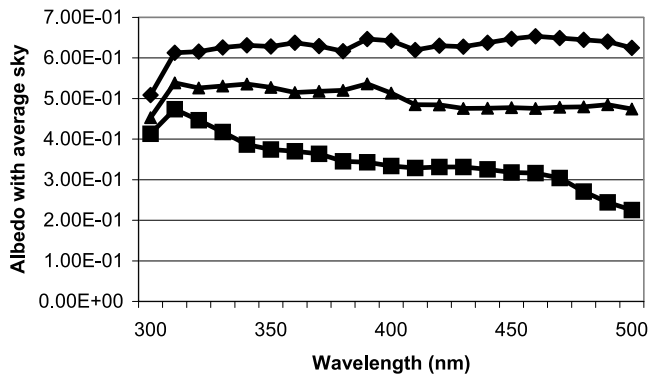

Figure 5. Cloud albedo calculated using average downwelling irradiance for complete cloud (diamonds), average of all measurements (triangles), and above long thin cloud gap (squares).

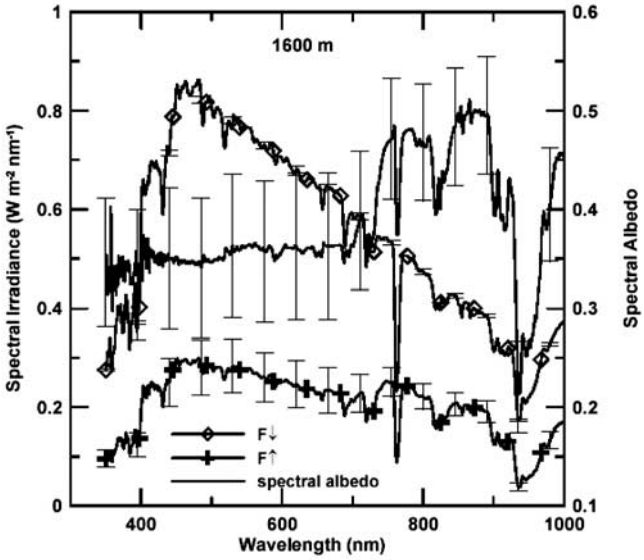

Figure 6. Averaged spectral downwelling and upwelling irradiance and spectral cloud top albedo of a stratocumulus measured at 1600 m altitude. Cloud top altitude is about 940 m.

leaving West Runton and flying in a SW direction toward Briston. It is near the coast where the cloud was most uniform and during that scan the aircraft did not pass over or adjacent to any gaps through which the ground could be seen. The bottom line in Figure 5 shows the opposite extreme, a scan taken at the Briston end of the flight path where the aircraft was flying entirely along a gap in the cloud aligned with the flight path. The cloud layer extended horizontally on either side of the gap so that the surface cover for the field of view of the down-pointing diffuser would look like a white circle (cloud) with a dark stripe down the middle (underlying arable land). Many of the other cloud albedo scans fluctuated between the upper and lower lines described above as the aircraft passed over occasional gaps in the cloud. The middle line in Figure 5 is the average albedo from all scans. There is no appreciable spectral dependence of the top line; the cloud was visually bright and white. As the ground surface occupies increasing amounts of the field of view, and therefore backscattering from 1520 m of atmosphere also plays a greater role, a spectral dependence becomes more apparent.

[35] The Partenavia was flying in the early afternoon of the same day (13 September) in horizontal flight legs around the measurement area at different altitudes. Example measurements are presented at 1600 m and 2800 m altitude for one short flight leg (5′) between the turning point in the SW and Aylsham in the SE. Figures 6 and 7 show averaged spectral upwelling and downwelling irradiances and the calculated cloud top albedo measured at two different altitudes (1600 and 2800 m), whereby the vertical bars indicate the standard deviation of the spectra. The SZAs of both flight legs were about 53.6° and 63.2°, respectively. For a better comparison all irradiances were converted to the same SZA of 63.2°. The influence of the surface vegetation below the cloud sheet is obvious by the strong increase of the spectral albedo bey 00 nm wavelength.

[36] Comparing Figures 6 and 7, a slight altitude dependence becomes apparent. The spectral cloud albedo decreases with increasing altitude, in particular for longer wavelengths. The reason for this albedo decrease is the increased downwelling irradiance because of the lower aerosol at higher altitudes. Thus the spectral cloud albedo (ratio of upwelling and downwelling irradiance) shows a tendency to decrease with increasing altitude. Moreover, the variability of the spectral cloud top albedo at 2800 m altitude is clearly smaller than at 1600 m (as can be seen from the standard deviations, i.e., the vertical bars). This is an effect of a smaller variability of the upwelling irradiance at higher altitudes as a greater surface area is viewed by the irradiance sensors which integrate over the hemisphere.

4.2.2. Homogeneous Cloud Layer

[37] On the following day (day 257, 14 September 2002) the albedometer on board the Partenavia aircraft was flown above a quite homogenous stratus cloud layer with no cloud gaps and with base heights around 460 m and cloud top altitudes at 980 m. Flights were conducted at the two altitudes 1600 m (i.e., 620 m above cloud top) and 2800 m (1800 m above cloud top) around the whole measurement area at nearly constant values of SZA (47.9°–51.7°). The upward and downward spectral flux densities and the resulting albedos are shown in Figures 8 and 9. As with the complete cloud data from the Cessna, there is only a slight wavelength dependence of the albedo within the wavelength range of the albedometer, even beyond 700 nm wavelength where gas absorption bands become apparent. Because of the compactness and high optical thickness of the stratus on this day the surface vegetation does not influence the spectral cloud albedo as it did for the scattered stratocumulus cloud case observed on 13 September.

[38] Compared with the scattered cloud layer (section 4.2.1) the same decrease in horizontal variability of albedo with altitude can be seen, and for the homogenous cloud

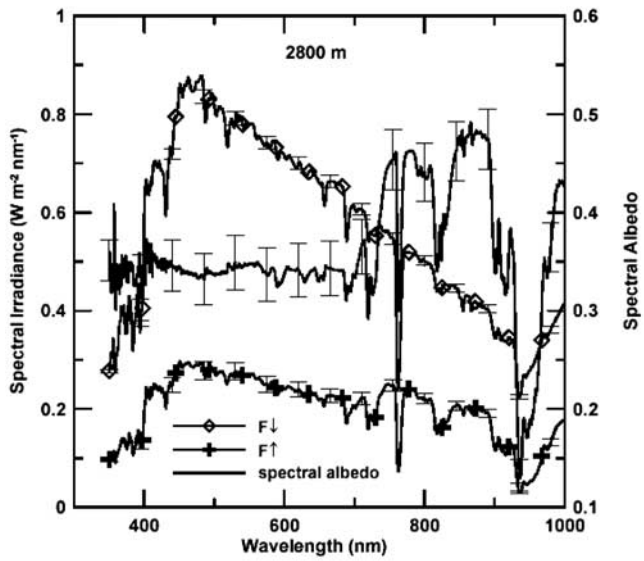

Figure 7. Averaged spectral downwelling and upwelling irradiance and spectral cloud top albedo of a stratocumulus measured at 2800 m altitude. Cloud top altitude is about 940 m.

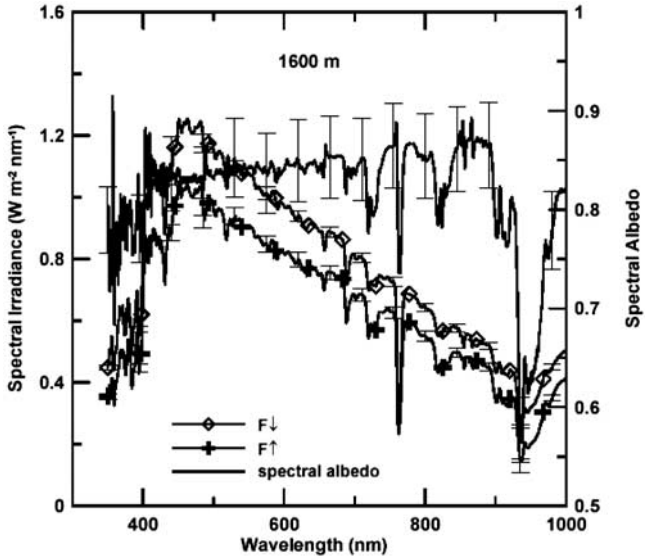

Figure 8. Averaged spectral downwelling and upwelling irradiance and spectral cloud top albedo of a homogeneous stratus layer measured at 1600 m altitude. Cloud top altitude is about 980 m.

there is a more pronounced decrease of albedo with altitude. This altitude dependence is not reproduced by the model simulations (Figure 10), in which the atmosphere is clean between the two flight altitudes and the decrease in albedo from 1600 m to 2800 m is small. The differences in the observed albedos at the two altitudes may be a result of large-scale horizontal cloud inhomogeneities. The aircraft travels a significant distance between making measurements at one altitude and ascending to make measurements at the next altitude, so it is sampling a different part of the cloud where microphysical and scattering properties (e.g. drop size distribution) may be different. This is supported by model simulations for various cloud optical thicknesses. These model simulations indicate that cloud horizontal inhomogeneities may well be the reason for the altitude dependence seen in the measurements.

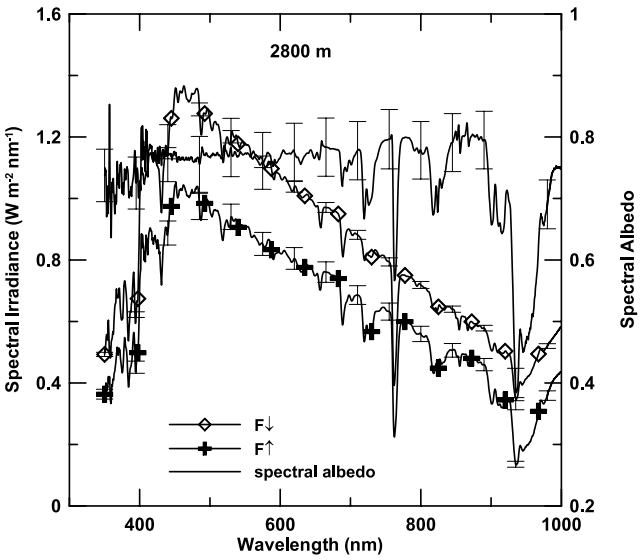

Figure 9. Averaged spectral downwelling and upwelling irradiance and spectral cloud top albedo of a homogeneous stratus layer measured at 2800 m altitude. Cloud top altitude is about 980 m.

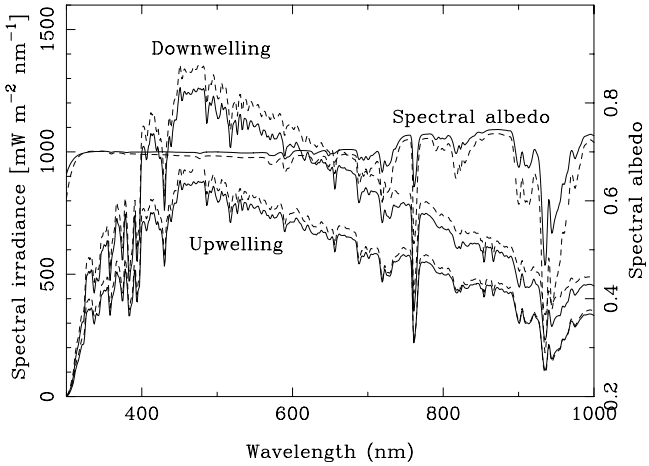

Figure 10. Model simulations of the downwelling and upwelling spectral irradiances measured at 1600 m (solid lines) and 2800 m (dashed lines) with corresponding spectral albedos.

5. Summary and Conclusions

[39] The spectral albedo for wavelengths from the UV (300 nm) to IR (1000 nm) has been measured from three airborne platforms in cloudless and cloudy conditions. Areal spectral albedo measurements from the NILU-CUBE and spectroradiometer on board the Cessna aircraft agree well where they coincide. The data were used to derive the spectral areal albedo of the surface beneath by linear extrapolation to the surface, a method that has proved valid in the clean air conditions experienced. The areal spectral albedo of the ground surface generally increased with wavelength through the UV and into the visible, while the albedo measured at certain altitudes above ground, incorporating atmospheric backscattering, showed a reversal in this tendency with height until albedo was decreasing with wavelength. Note that these results are specific to flat farmland and relatively clean air conditions. Different ground surfaces and/or, a more turbid atmosphere would produce different results and the linear extrapolation method is not suitable for use in high aerosol conditions.

[40] In addition, the spectral albedo of broken and uniform cloud layers has been derived from the measurements. The albedo of broken and closed stratocumulus cloud layers was measured from both the Cessna and Partenavia and found to be independent of wavelength at UV and visible wavelengths. Gaps in the broken cloud case decreased the cloud albedo and produced obvious surface reflectance signatures in the averaged albedo spectra measured above the broken cloud. The measured albedo above the cloud decreased with measurement altitude due to increasing downwelling radiation and increased attenuation of the upwelling radiation from a highly reflective surface.

[41] **Acknowledgments.** The INSPECTRO campaign was funded by the European Commission EVKT2-2001-00130, and provided support for the participation of UMIST and NILU. Funding by the German Science Foundation (DFG) is acknowledged for the contribution of the Leipzig group. Ian Stromberg and John Rimmer contributed to the successful operation of the Cessna. Sebastian Schmidt is acknowledged for his contributions to the albedometer measurements. The enviscope GmbH company and the pilot of the Partenavia, Bernd Schumacher, did an excellent job in preparing and conducting the measurements with the Partenavia. Jost Heintzenberg (IfT) has continuously supported this work. Mario Blumthaler (University of Innsbruck) and Stelios Kazadzidis (University of Thessaloniki) operated the spectroradiometers referred to in the intercomparisons at Weybourne and Norwich Airport. Part of this research was performed while one of the authors (MW) held a National Research Council Research Associateship Award at the NASA Ames Research Center.

References

Anderson, G., S. Clough, F. Kneizys, J. Chetwynd, and E. Shettle (1986), AFGL atmospheric constituent profiles (0–120 km), *Tech. Rep. AFGL-TR-86-0110*, Air Force Geophys. Lab., Hanscom Air Force Base, Bedford, Mass.

Bass, A. M., and R. J. Paur (1985), The ultraviolet cross-section of ozone, I, The measurements, in *Atmospheric Ozone: Proceedings of the Quadrennial Ozone Symposium*, edited by C. S. Zerefos and A. Ghazi, pp. 601–606, D. Reidel, Norwell, Mass.

Dahlback, A. (1996), Measurements of biologically effective UV doses, total ozone abundances, and cloud effects with multichannel, moderate bandwidth filter instruments, *Appl. Opt.*, *35*, 6514–6521.

Dahlback, A., and K. Stamnes (1991), A new spherical model for computing the radiation field available for photolysis and heating at twilight, *Planet. Space Sci.*, *39*, 671–683.

Degünther, M., and R. Meerkötter (2000), Effect of remote clouds on surface UV irradiance, *Ann. Geophys.*, *18*, 679–686.

Degünther, M., R. Meerkötter, A. Albold, and G. Seckmeyer (1998), Case study on the influence of inhomogeneous surface albedo on UV irradiance, *Geophys. Res. Lett.*, *25*, 3587–3590.

Feister, U., and R. Grewe (1995), Spectral albedo measurements in the UV and visible region over different types of surfaces, *Photochem. Photobiol.*, *62*, 736–744.

Hofzumahaus, A., A. Kraus, A. Kylling, and C. Zerefos (2002), Solar actinic radiation (280–420 nm) in the cloud-free troposphere between ground and 12 km altitude: Measurements and model results, *J. Geophys. Res.*, *107*(D18), 8139, doi:10.1029/2001JD900142.

Høiskar, B. A. K., R. Haugen, T. Danielsen, A. Kylling, K. Edvardsen, A. Dahlback, B. Johnsen, M. Blumthaler, and J. Schreder (2003), Multichannel moderate-bandwidth filter instrument for measurement of the ozone-column amount, cloud transmittance, and ultraviolet dose rates, *Appl. Opt.*, *42*, 3472–3479.

Hu, Y. X., and K. Stamnes (1993), An accurate parameterization of the radiative properties of water clouds suitable for use in climate models, *J. Clim.*, *6*, 728–742.

Jäkel, E., M. Wendisch, A. Kniffka, and T. Trautmann (2004), A new airborne system for fast measurements of up- and downwelling spectral actinic flux densities, *Appl. Opt.*, in press.

Kylling, A., A. F. Bais, M. Blumthaler, J. Schreder, C. S. Zerefos, and E. Kosmidis (1998), The effect of aerosols on solar UV irradiances during the Photochemical Activity and Solar Ultraviolet Radiation campaign, *J. Geophys. Res.*, *103*, 26,051–26,060.

Kylling, A., T. Danielsen, M. Blumthaler, J. Schreder, and B. Johnsen (2003), Twilight tropospheric and stratospheric photodissociation rates derived from balloon borne radiation measurements, *Atmos. Chem. Phys.*, *3*, 377–385.

Mayer, B., and M. Degünther (2000), Comment on ''Measurements of erythemal irradiance near Davis Station, Antarctica: Effect of inhomogeneous surface albedo,'' *Geophys. Res. Lett.*, *27*, 3489–3490.

Mayer, B., G. Seckmeyer, and A. Kylling (1997), Systematic long-term comparison of spectral UV measurements and UVSPEC modeling results, *J. Geophys. Res.*, *102*, 8755–8767.

McKenzie, R. L., and M. Kotkamp (1996), Upwelling UV spectral irradiances and surface albedo measurements at Lauder, New Zealand, *Geophys. Res. Lett.*, *23*, 1757–1760.

Stamnes, K., S.-C. Tsay, W. Wiscombe, and K. Jayaweera (1988), Numerically stable algorithm for discrete-ordinate-method radiative transfer in multiple scattering and emitting layered media, *Appl. Opt.*, *27*, 2502–2509.

Webb, A. R., I. M. Stromberg, H. Li, and L. M. Bartlett (2000), Airborne spectral measurements of surface reflectivity at ultraviolet and visible wavelengths, *J. Geophys. Res.*, *105*, 4945–4948.

Webb, A. R., et al. (2002), Measuring spectral actinic flux and irradiance: Experimental results from the ADMIRA (Actinic Flux Determination from Measurements of Irradiance), *J. Atmos. Oceanic Technol.*, *19*, 1049–1062.

Wendisch, M., and B. Mayer (2003), Vertical distribution of spectral solar irradiance in the cloudless sky—A case study, *Geophys. Res. Lett.*, *30*(4), 1183, doi:10.1029/2002GL016529.

Wendisch, M., D. Müller, D. Schell, and J. Heintzenberg (2001), An airborne spectral albedometer with active horizontal stabilization, *J. Atmos. Oceanic Technol.*, *18*, 1856–1866.

Wendisch, M., P. Pilewskie, E. Jäkel, S. Schmidt, J. Pommier, S. Howard, H. H. Jonsson, H. Guan, M. Schröder, and B. Mayer (2004), Airborne measurements of areal spectral surface albedo over different sea and land surfaces, *J. Geophys. Res.*, *109*, D08203, doi:10.1029/2003JD004392.

E. Jäkel, Leibniz-Institute for Tropospheric Research (IfT), Permosestrasse 15, D-04318 Leipzig, Germany. (jaekel@tropos.de)

A. Kylling, Norwegian Institute for Air Research (NILU), P.O. Box 100, N-2027 Kjeller, Norway. (arve.kylling@nilu.no)

A. R. Webb, Physics Department, University of Manchester Institute of Science and Technology (UMIST), Sackville Street, Manchester M60 1QD, UK. (ann.webb@umist.ac.uk)

M. Wendisch, NASA Ames Research Center, MS 245-4, Moffett Field, CA 94035, USA. (mwendisch@mail.arc.nasa.gov)